Available online at www.sciencedirect.com

ScienceDirect

Ceramics International 40 (2014) 2565–2573

CERAMICS INTERNATIONAL

www.elsevier.com/locate/ceramint

Review paper

Eutectic crystallization in the UO_2–Al_2O_3–HfO_2 ceramic phase diagram

K. Plevacova[a], C. Journeau[a], P. Piluso[a], J. Poirier[b,*]

[a]CEA, DEN, STRI, LMA, Cadarache, 3108 St. Paul lez Durance, France
[b]CEMHTI, 1D, av de la Recherche Scientifique, 45071 Orléans Cedex 2, France

Received 13 July 2013; accepted 9 August 2013
Available online 7 September 2013

Abstract

In the frame of the Generation IV Sodium Fast Reactor (SFR) safety studies, a core catcher with a sacrificial material could be placed at the bottom of the nuclear reactor. Its role is to dilute the (U, Pu)O_2 molten fuel in case of a hypothetical core meltdown accident. A Al_2O_3–HfO_2 ceramic is a candidate for the sacrificial material. To understand how the molten fuel would mix with this sacrificial material, the UO_2–Al_2O_3–HfO_2 system was investigated at CEA Cadarache PLINIUS corium platform. The eutectic position of the UO_2–Al_2O_3–HfO_2 was determined: the eutectic temperature is 1728 ± 22 °C (2001 ± 22 K) and the eutectic composition is 30 wt% UO_2–35 wt% Al_2O_3–35 wt% HfO_2. Then, the pseudo-binary UO_2–(50 wt% Al_2O_3–50 wt% HfO_2) phase diagram has been proposed.

Keywords: Ceramic phase diagram; UO_2–Al_2O_3–HfO_2; Eutectic position; Generation IV nuclear reactor; Core catcher

Contents

*Corresponding author. Tel.: +33 2 38 25 55 14; fax: +33 2 38 63 81 03.
E-mail addresses: jacques.poirier@univ-orleans.fr, Poirierja@wanadoo.fr (J. Poirier).

0272-8842/$ - see front matter © 2013 Elsevier Ltd and Techna Group S.r.l. All rights reserved.
http://dx.doi.org/10.1016/j.ceramint.2013.08.047

1. Introduction

In order to increase the safety of Generation IV Sodium Fast Reactors (SFR), hypothetical severe accidents have to be investigated and their consequences must be limited [1]. In case of a hypothetical core meltdown accident in the reactor, a multiphase and multiconstituent melt, called corium, could form. It is composed of the (U, Pu)O_2 molten fuel, stainless steel and zircaloy coming from the core structures and cladding. The corium is a very complex and chemical aggressive mixture, its temperature can reach 2800 °C. To mitigate severe accidents of future sodium fast reactors, a core catcher will be installed. Its role is to contain corium and to stabilize it to avoid the release of radioactive materials into the environment. To design a robust core catcher, sacrificial ceramic materials are likely to be introduced in it. These ceramic materials should mix with the fissile part of the corium and dilute it. By dilution, the recriticality risk should be removed while adding the thermal protection of the core catcher structures.

The Al_2O_3–HfO_2 mixture may be chosen as a sacrificial ceramic material for the core catcher, in which Hf will provide some neutron absorption [2–4]. To forecast the behavior of the molten fuel when in contact with the sacrificial material, it is necessary to know the UO_2–Al_2O_3–HfO_2 phase diagram.

Indeed, in this study, (U, Pu)O_2 fuel will be identified as UO_2. This simplification is admissible in a first approach since the SFR fuel should contain only about 15 wt% of PuO_2 and both oxides have relatively similar chemical behaviors.

To obtain a maximum dilution of corium at a minimum temperature, the ternary eutectic point has been investigated; the aim is to use these data to define the composition and the temperature of this ternary eutectic point and to deduce the optimal chemical composition of the sacrificial material.

The study of the Al_2O_3–HfO_2 system and its interaction with UO_2 has been performed in France within the CEA Cadarache severe accident mastering experimental laboratory [2]. To the authors' knowledge the ceramic phase diagram of the ternary system UO_2–Al_2O_3–HfO_2 has not been fully investigated to date. Only the binary diagrams UO_2–Al_2O_3 and Al_2O_3–HfO_2 have been published [5–7].

The ceramic phase diagram of the UO_2–Al_2O_3 system was studied by Lambertson et al. [7] and by Epstein et al. [8]. Both authors agree on the existence of a unique eutectic point for about 52 wt% of Al_2O_3 at 1915 ± 15 °C. But contrary to Epstein et al., Lambertson et al. reported a miscibility gap formation between 24 and 53 wt% of Al_2O_3.

According to Lopato et al. [6], the Al_2O_3–HfO_2 system is also a system with only one eutectic position for 50 ± 3 wt% of Al_2O_3 at 1890 °C.

The primary aim of the present study is to consider the whole system and to find its ternary eutectic position experimentally. First, the materials and methods used are presented. Then, the experiments performed in the relevant binary and ternary ceramic systems are described and discussed. The results of these experiments allow proposing the ternary UO_2–Al_2O_3–HfO_2 eutectic composition and temperature.

2. Materials and methods

2.1. UO_2, Al_2O_3, HfO_2 materials

The experiments use the so-called "prototypic corium" in which the (U, Pu)O_2 fuel is simulated by depleted UO_2 in contact with the Al_2O_3–HfO_2 sacrificial material.

These oxides have very high fusion temperatures: T_f (UO_2) = 2847 °C, T_f (Al_2O_3) = 2042 °C, T_f (HfO_2) = 2850 °C [6,7].

The UO_2, Al_2O_3, HfO_2 samples were prepared from oxide powders: depleted (0.22 wt% of ^{235}U), 99.9 wt% pure UO_2 industrial powder; 99.99 wt% pure Al_2O_3 powder from Alfa Aesar; 99.9 wt% pure HfO_2 powder from CEZUS. The powders were mixed together in a mortar for 10 min and then introduced into the crucible. 8–10 g of mixture is prepared for each test.

2.2. Apparatus

The experiments on the UO_2–Al_2O_3–HfO_2 system were performed at the CEA Cadarache PLINIUS experimental platform, in the VITI facility [9–11]. The VITI facility has been developed to study chemical interactions between different ceramic materials at high temperature and to measure viscosity, density and surface tension on corium up to 2600 °C by aerodynamic levitation. The facility, used to study the eutectic crystallization of the UO_2–$Al2O_3$–HfO_2, is represented in Fig. 1.

The working chamber volume is of about 70 L. It is possible to work either under low vacuum or under inert gas atmosphere. The maximum absolute pressure in the working chamber is 2.5×10^5 Pa. Induction heating is used to reach temperatures above 2000 °C with limited thermal gradient. The induction coil couples with a graphite susceptor, which heats the crucible by thermal radiation. The radiation losses are attenuated by a dedicated thermal shield. The maximum

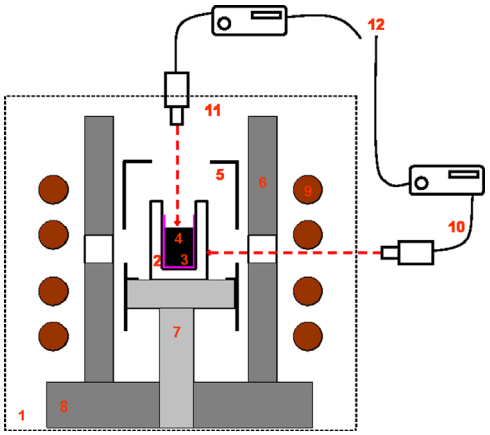

Fig. 1. Scheme of VITI furnace. (1) VITI tank, (2) crucible, (3) protective coating (option), (4) mixture, (5) graphite susceptor, (6) thermal shield, (7) support for crucible, (8) support for thermal shield, (9) inductance coil, (10) pyrometer, measurement of $T_{mixture}$, (11) pyrometer, measurement of $T_{crucible}$, (12) data acquisition.

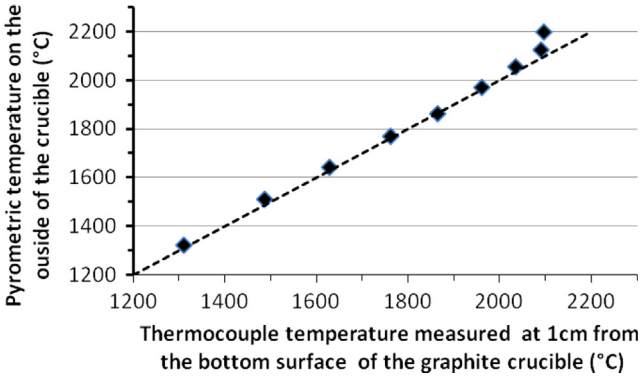

Fig. 2. Calibration of pyrometric temperature by thermocouple measurements.

electrical power of the induction generator is 24 kW and its frequency is 23 kHz.

The temperature of the studied material mixture and the temperature of the external crucible wall are measured by two IMPAC-ISQ-LO bichromatic pyrometers ($\lambda_1 = 0.92$ and $\lambda_2 = 1.04$ μm). The temperature measurement is based on the ratio of the radiation signals of two adjacent wavelengths. Gray bodies, i.e., targets with the same emissivity on both wavelengths, can be measured without emissivity setting.

The two channels pyrometers have a temperature range of 1250–3300 °C. The measurement uncertainty (manufacturer's data) is ± 35 °C.

– The outside temperature of the crucible is measured through a small window in the graphite susceptor (see Fig. 1), which is similar to a black body with a cylindrical geometry. The apparent emissivity of the graphite for a non-spherical cavity is given by Gouffé's formula [12]:

$$\varepsilon_g = \frac{1}{1+((1/\varepsilon_S)-1)(A_0/4\pi\, a^2)}[1+(1-\varepsilon_S)((A_0/S)-(A_0/\pi l^2))]$$

with A_0 as the area of the orifice (window) (= 80 mm^2), a the radius of the cavity (= 24 mm), S the surface of the cavity (= 17,000 mm^2), l the height of the cavity (= 100 mm), and ε_s the emissivity of the material of the cavity (graphite).

The ratio of emissivity (at 0.90 μm and 1.04 μm wavelengths) is very close to 1.

– The temperature of the studied mixture was measured directly by the top of the crucible. At temperatures of the test (1200–2200 °C), the studied mixture is not a black body. its emissivity is not close to 1. However, the ratio of emissivity (at 0.90 μm and 1.04 μm wavelengths) is very close to 1 [12].

Thus, the uncertainty of the temperature measurement related to the graphite material and the studied mixture are negligible.

The temperatures of pyrometers were calibrated by thermocouple measurements.

A (tungsten, rhenium) C type thermocouple was positioned 1 cm from the bottom surface of the graphite crucible. Fig. 2 shows the temperatures measured by pyrometer in relation to the temperature measured by thermocouple (test performed without a liquid oxide mixture). The temperatures obtained by the pyrometers are extremely close with those obtained by the thermocouples to a temperature of 2200 °C (difference < 1%).

The homogeneity of the furnace temperature in the area of the graphite susceptor was also measured. Temperatures are homogeneous at +/− 4 °C.

2.3. Experimental procedure

The experiments related to our study were performed with an absolute pressure of the working chamber of 1.8×10^5 Pa. Graphite crucibles with a protective zirconium carbide coating, (which avoids the reduction of graphite by UO_2 [13,14]) or tungsten crucibles were used to contain the studied mixtures. The samples were heated until completed melted and then they were cooled down very quickly (500 °C/min) when the generator was switched off. The mixtures were exposed to an argon furnace atmosphere (under a 5 L/min argon flow) to avoid the change of UO_2–Al_2O_3–HfO_2 composition due to the potential of oxygen. The risk of vaporization of oxides during the test is very low considering their very high boiling temperature: T_b UO_2=4100 °C, T_b HfO_2=5400 °C, T_b Al_2O_3=2980 °C, T_b Al_2O_3–HFO_2 eutectic point > 2850 °C [2].

The experimental method is a thermal analysis in which the temperature of a phase change is determined from changes in the rate of cooling or heating brought about by the heat of reaction.

The eutectic temperature of our different mixtures was measured during the cooling. Indeed, a solidification plateau appears on the temperature curve of the mixture at eutectic temperature (Fig. 3). When the UO_2–(50 wt% Al_2O_3–50 wt% HfO_2) phase diagram was investigated, its liquidus temperatures were also determined from cooling curves: at liquidus temperature, a change of slope was observed.

The experimental conditions of different performed experiments related to the UO_2–Al_2O_3–HfO_2 system study are gathered in Table 1.

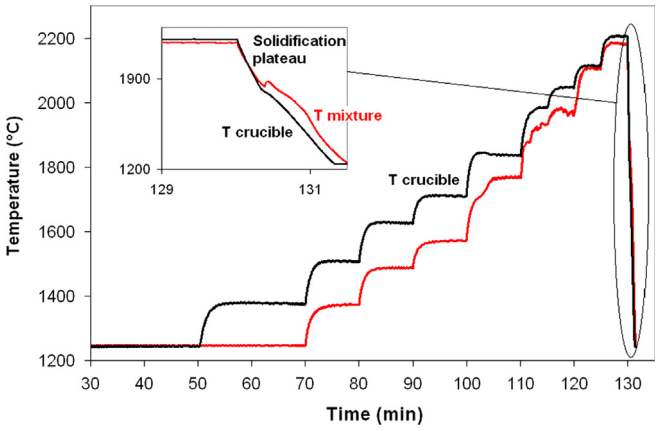

Fig. 3. The recorded temperature curves related to the Al_2O_3–UO_2 experiment performed in the tungsten crucible. During the cooling stage, the temperature curve of the mixture shows a solidification plateau at 1880 °C.

Table 1
Description of different experiments performed in the frame of the UO_2–Al_2O_3–HfO_2 system study (The objective of each experiment is indicated).

System	Crucible	Initial composition (wt%)	Objective
Al_2O_3	Tungsten	100% Al_2O_3	To evaluate the reliability of the experimental data
UO_2–Al_2O_3	C_{gr}+ZrC	48% UO_2–52% Al_2O	To verify the eutectic position
	Tungsten	60% UO_2–40% Al_2O	To verify the absence of the miscibility gap
Al_2O_3–HfO_2	Tungsten	50% Al_2O_3–50% HfO_2	To verify the eutectic position
UO_2–Al_2O_3–HfO_2	Tungsten	31% UO_2–34% Al_2O_3–35% HfO_2	To determine the eutectic position
		40% UO_2–30% Al_2O_3–30% HfO_2	To investigate the pseudo-binary UO_2–(50 wt% Al_2O_3–50 wt% HfO_2) phase diagram
		60% UO_2–20% Al_2O_3–20% HfO_2	
		70% UO_2–15% Al_2O_3–15% HfO_2	

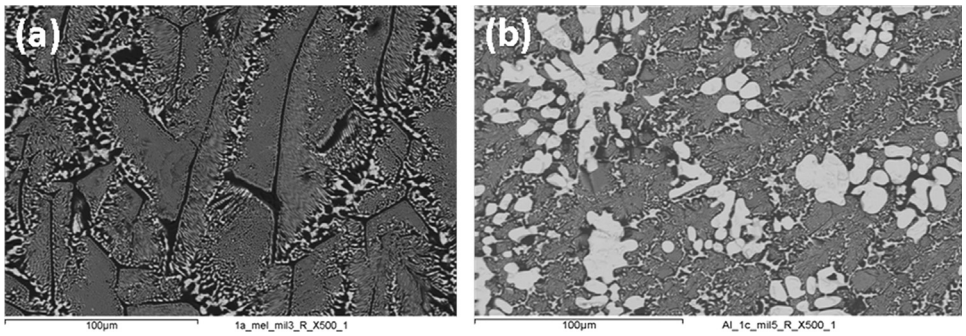

Fig. 4. Back-scattered scanning electron micrographs (500×) of the UO_2+Al_2O_3 mixtures, Black ≈ Al_2O_3, white ≈ UO_2. (a) 48 wt% UO_2+52 wt% Al_2O_3 mixture heated in a ZrC-coated graphite crucible. The eutectic phase composition determined by EDS is 47 wt% UO_2+53 wt% Al_2O_3. (b) 60 wt% UO_2+40 wt% Al_2O_3 mixture heated in a tungsten crucible. Dendrites of proeutectic UO_2 and eutectic phase formed. There is no miscibility gap.

A scanning electron microscopy (CAMBRIDGE S360 SEM) equipped with an energy-dispersive X-ray spectrometer (OXFORD EDS 7060 analyzer) was used for the microstructural analysis of samples. Each chemical analysis has, on average, over five measurements at least. Uncertainty of measurements is less than 10% for metallic elements (Al,HF, U) [15]. X-ray diffraction (SIEMENS D5000 XRD diffractometer in the Bragg–Brentano configuration) helped to complete the information about the crystallized phases.

3. Results and discussion

The experimental results are presented as an increasingly complexity of Al_2O_3, UO_2, HfO_2 system:

– melting temperature of Al_2O_3 pure compound;
– binary eutectic in UO_2–Al_2O_3 and Al_2O_3–HfO_2 systems; and
– ternary eutectic in UO_2–Al_2O_3–HfO_2 system.

3.1. Melting temperature of Al_2O_3 pure compound

The pure alumina powder was heated up to 2200 °C in a tungsten crucible. During cooling, the temperature of the alumina measured on the top of the crucible presents a plateau. This plateau is due to the change of the liquid to solid state of alumina, at a constant temperature. The solidification temperature of pure alumina measured is 2030 °C. This temperature is close to the temperature reported by the literature: 2042 °C [6].

3.2. Binary eutectic in Al_2O_3–UO_2 and Al_2O_3–HfO_2 systems

3.2.1. UO_2–Al_2O_3 system

Two experiments within the UO_2–Al_2O_3 system were performed in order to verify the eutectic position and to verify the miscibility gap existence (Table 1).

The eutectic temperature was measured during the cooling of the samples (presence of a solidification plateau). The recorded temperature curves related to the experiment performed in a tungsten crucible shows a solidification plateau on the temperature curve of the 40 wt% Al_2O_3–60 wt% UO_2 mixture during the cooling stage (Fig. 3). The experimental average value of the eutectic temperature is 1850 °C.

Fig. 4 shows the two crystallized phases (proeutectic UO_2 phase and eutectic UO_2–Al_20_3 phase) of the studied mixtures after melting and cooling. The eutectic phase has a characteristic fine lamellar microstructure.

The composition of the eutectic phase was determined by EDS: 47 wt% UO_2+53 wt% Al_2O_3 (Fig. 4(a)), which matches well with the composition found in the literature (48 wt% UO_2+52 wt% Al_2O_3) within the analysis uncertainties of 5 wt%.

The XRD analysis of the crystallized samples confirmed the presence of UO_2 and Al_2O_3.with a little pollution of tungsten oxides from crucible (Fig. 5).

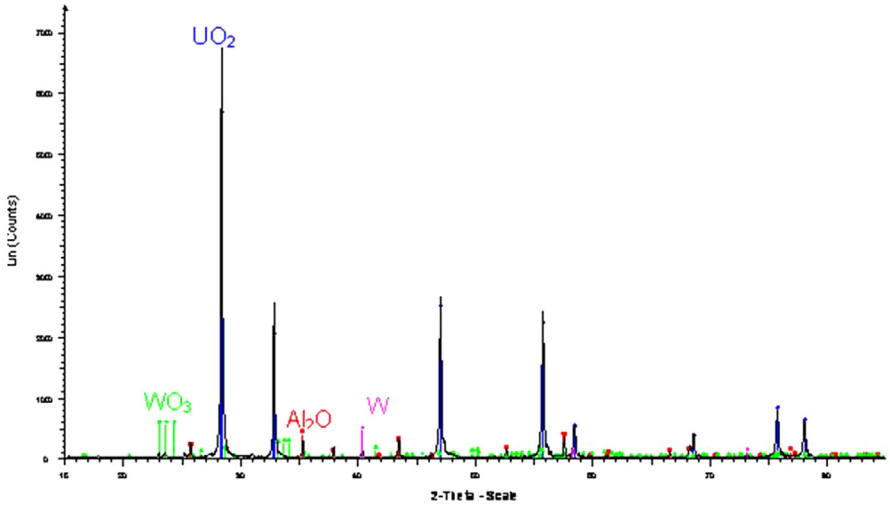

Fig. 5. X-ray diffraction of 40 wt% Al_2O_3–60 wt% UO_2 sample.

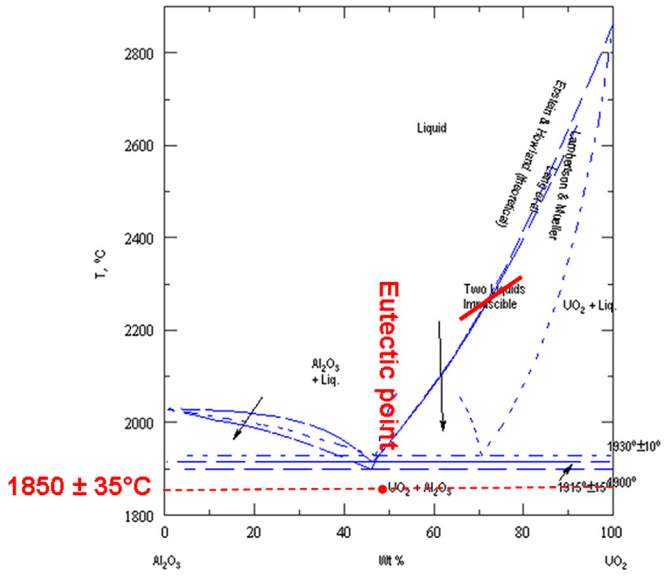

Fig. 6. Modified $UO_2+Al_2O_3$ phase diagram from [5] after our experiments. The eutectic was found almost for the same composition but for a lower temperature: 47 wt% UO_2+53 wt% Al_2O_3 and 1850 ± 35 °C. No miscibility gap was observed in this system.

The existence of the miscibility gap at liquid state was invalidated by the experiment with the 40 wt% Al_2O_3–60% wt % UO_2 hypereutectic composition.

After the crystallization of the melt, a mixture of eutectic phase and proeutectic UO_2 are formed (Fig. 4(b)). Guéneau et al. [16] studied the miscibility gaps in the diagrams O–U and O–U–Zr. The typical morphology of a miscibility gap is made of immiscible droplets in a matrix. For the 60 Wt% UO_2–40 wt % Al_2O_3 mixture, typical morphologies of a miscibility gap were not observed. It is thus possible to conclude that UO_2–Al_2O_3 are miscible, confirming the results of Epstein et al. [8].

The eutectic position determined during our experiments is represented on the phase diagram published by Lang et al. [5], in Fig. 6. The measured eutectic temperature is 65 °C lower than the temperature found in the literature (1915 ± 15 °C).

3.2.2. Al_2O_3–HfO_2 system

An experiment with the 50 wt% HfO_2–50 wt% Al_2O_3 initial mixture was carried out to verify the eutectic position. The SEM micrographs (Fig. 7) show a very fine eutectic lamellar phase formed everywhere in the sample after its crystallization. Its composition measured by EDS: 49 wt% HfO_2–51 wt% Al_2O_3 is consistent with the composition: 50 wt% HfO_2–50 wt % $Al_2O_3\pm3$% found in the literature [6].

The XRD analysis of the sample confirmed the presence of only HfO_2 and Al_2O_3 phases (Fig. 8).

The experimental eutectic temperature was measured during the cooling of the sample. The eutectic temperature is 1800 °C. The new HfO_2–Al_2O_3 eutectic point is positioned on the HfO_2–Al_2O_3 phase diagram established by Lopato et al. [6] (Fig. 9). The measured eutectic temperature is a little lower than the temperatures of the literature.

3.3. Ternary eutectic in UO_2–Al_2O_3–HfO_2 system

The UO_2–Al_2O_3–HfO_2 ternary phase diagram has never been studied. Each binary UO_2–Al_2O_3 and Al_2O_3–HfO_2 diagrams have only one eutectic point. Therefore, the UO_2–Al_2O_3–HfO_2 phase diagram has two eutectic valleys which converge to a ternary eutectic point whose composition is not known.

3.3.1. Thermodynamic calculations

GEMINI2 software coupled to the thermodynamic database NUCLEA_O8 database [15] were used to determine the chemical composition of the ternary eutectic point in the UO_2–Al_2O_3–HfO_2 system.

GEMINI2 (Gibbs Energy MINImizer) software, based on the principle of total Gibbs's energy minimization, is well adapted to determine the equilibrium in complex chemical systems, such as corium [17]. The NUCLEA_O8 database was developed in the frame of severe accident research for Pressurized Water Reactors.

UO_2 and Al_2O_3 are part of this database, while HfO_2 is not present. It was nevertheless possible to replace a mole of HfO_2

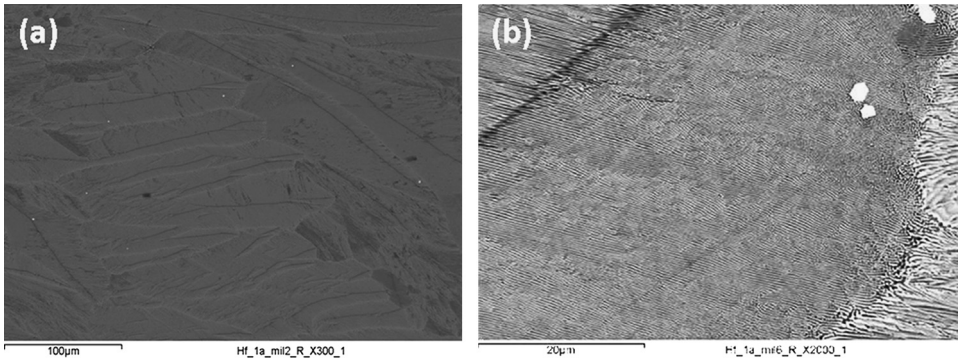

Fig. 7. Back-scattered scanning electron micrographs of the 50 wt% HfO_2+50 wt% Al_2O_3 mixture heated in a tungsten crucible, Gray ≈ Al_2O_3, White ≈ HfO_2. Only one eutectic phase formed. Its composition determined by EDS is 49 wt% HfO_2+51 wt% Al_2O_3.(a) 300 × and (b) 2000 × .

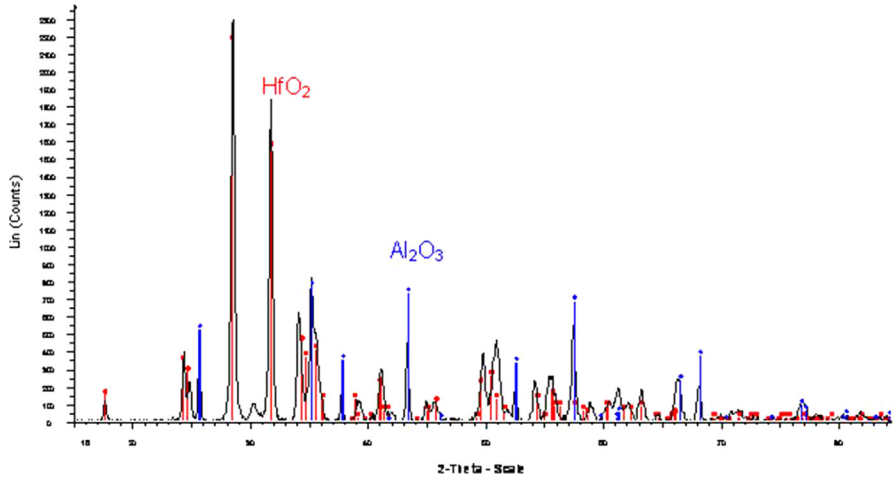

Fig. 8. X-ray diffraction of 50 wt% HfO_2+50 wt% Al_2O_3 sample.

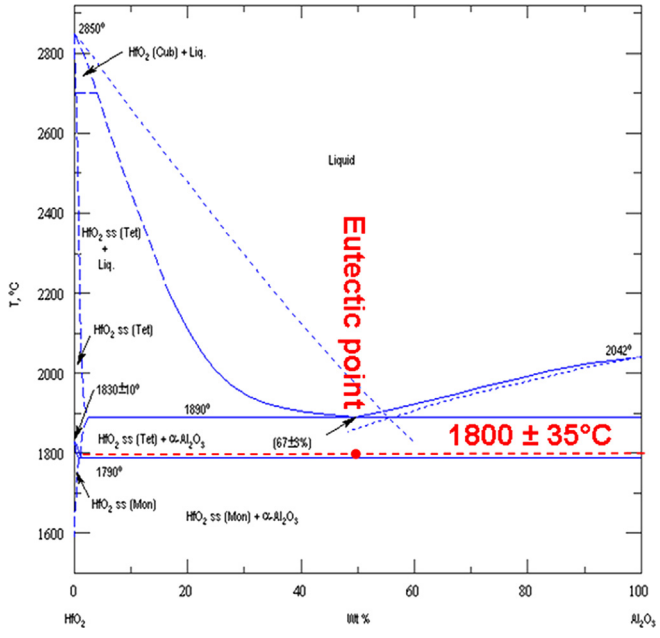

Fig. 9. Modified UO_2+Al_2O_3 phase diagram from [6] after our experiments. The eutectic was found almost for the same composition but for a lower temperature: 49 wt% HfO_2+51 wt% Al_2O_3 and 1800 ± 35 °C.

by a mole of ZrO_2. Indeed, HfO_2 and ZrO_2 have close chemical behavior since they have the same crystalline structure, the same allotropic transformations and since the ionic radii of Hf^{4+} and Zr^{4+} are very close (respectively 0.83 and 0.84×10^{-10} m).

A GEMINI2 calculation is made using these initial proportions, replacing a mole of HfO_2 by a mole of ZrO_2.

GEMINI2 calculations are interpolated from the corresponding ternary and binary systems and their thermodynamic properties included in the NUCLEA_08 database. The quality criteria for binary and ternary sub-systems included in the UO_2–Al_2O_3–ZrO_2 system, based on comparisons between calculation and available experimental data, are considered as acceptable, which means that these systems are well known and satisfactorily modeled.

Fig. 10 represents the temperature evolution of the weight fraction of different materials of this UO_2–Al_2O_3–ZrO_2 ternary system. According to this figure, the solid solution $(U_{1-x}Zr_x)O_2$ and Al_2O_3 melt simultaneously at constant temperature.

The UO_2–HfO_2 indifferent point position, characterizing the transformation of the $(U_{1-x}Hf_x)O_2$ solid solution from solid state to liquid state at constant composition and temperature, was estimated at 54 wt% HfO_2, by analogy with the (UO_2–ZrO_2)

pseudo-binary diagram. The ternary eutectic composition was estimated at 31 wt% of UO_2, 34 wt% of Al_2O_3 and 35 wt% of HfO_2.

The thermodynamic calculations confirm the estimated eutectic composition. Nevertheless, this composition needs to be experimentally verified.

3.3.2. Experimentations

First, the experiment within the UO_2–Al_2O_3–HfO_2 system was performed with the composition estimated by GEMINI2 software coupled to NUCLEA_O8 database: 31 wt% UO_2–34 wt% Al_2O_3–35 wt% HfO_2. The micrograph of this sample after melting and crystallization (Fig. 11(a)) shows that a fine eutectic phase formed. The ternary eutectic composition was determined by EDS as 30 wt% UO_2–35 wt% Al_2O_3–35 wt% HfO_2, which confirms the GEMINI2 estimation within the 3 wt% uncertainty.

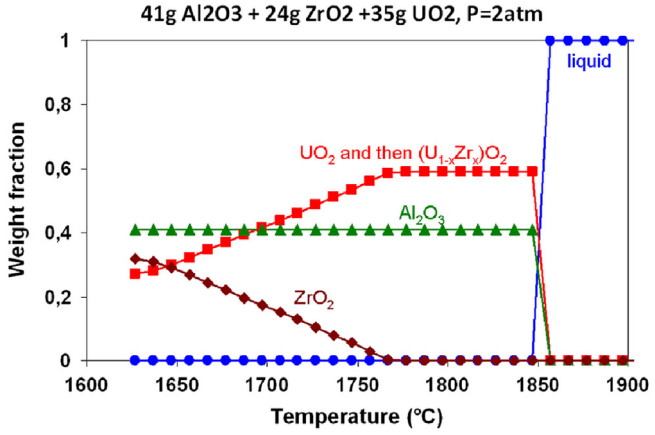

Fig. 10. GEMINI2 and NUCLEA_08 calculation simulating 35 wt% UO_2–41 wt% Al_2O_3–24 wt% ZrO_2 interaction. On the graph, weight fractions are plotted against the temperature. The initial composition of oxides was determined considering UO_2–Al_2O_3 and Al_2O_3–HfO_2 eutectic composition ratios and replacing a mole of HfO_2 by a mole of ZrO_2.

Then, the pseudo-binary UO_2–(50 wt% Al_2O_3–50 wt% HfO_2) phase diagram was studied. Indeed, in case of a hypothetical core melt-down accident, the amount of UO_2 varies in the core catcher, whereas the wt% Al_2O_3/wt% HfO_2 ratio remains a constant characteristic of the chosen sacrificial material. Thus, three other ternary mixtures were considered, with 40 wt% UO_2, 60 wt% UO_2 and 70 wt% UO_2.

The SEM micrographs of these hypereutectic mixtures after crystallization are shown in Fig. 11(b–d). As expected, the proportion of proeutectic UO_2 dendrites increases with the initial UO_2 fraction. According to the EDS analysis, there is HfO_2 solubility in these UO_2 dendrites up to 10 wt%. The eutectic zones were composed of Al_2O_3 and of $(U_{1-x}Hf_x)O_2$ solid solution lamellas, with some solubility of HfO_2 in UO_2. This solid solution was detected by EDS, but also by XRD.

The XRD characterization reveals the presence of three phases: Al_2O_3, HfO_2 and a $(U_{1-x}Hf_x)$ O_2 solid solution (Fig. 12). The lattice parameter of the $(U_{1-x}Hf_x)$ O_2 solid solution decreases when the fraction of hafnium increases in accordance with linear Vegard's law [18].

Table 2 presents the eutectic temperatures, the liquidus temperatures and the eutectic compositions determined from the temperature measurements recorded during cooling and from the EDS analysis of microstructures of the four ternary mixtures. Only the composition of eutectic zones of the UO_2

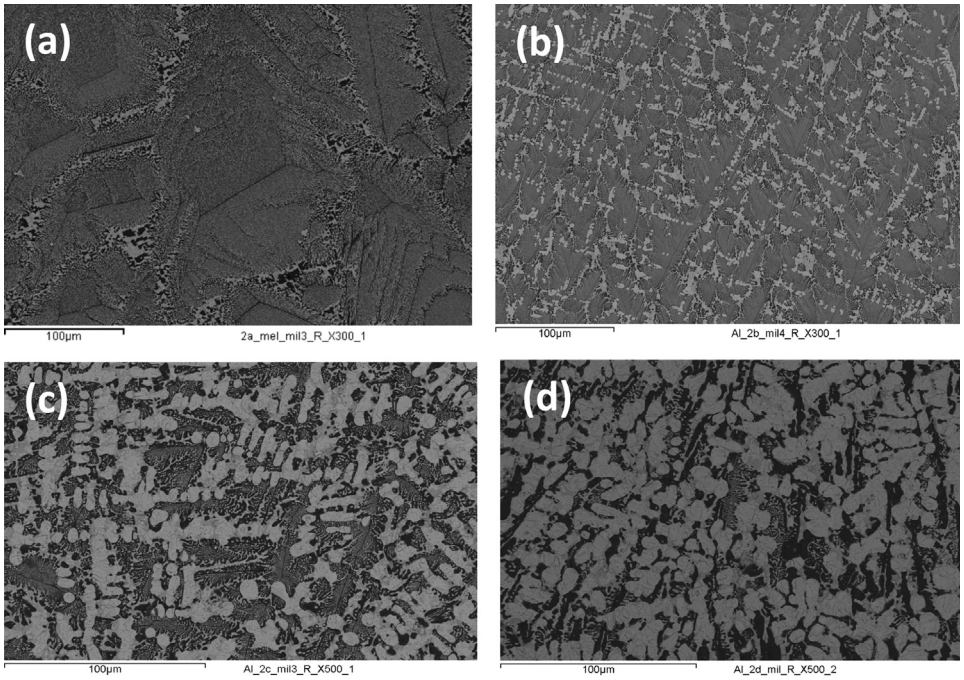

Fig. 11. Back-scattered scanning electron micrographs (300 ×) of the UO_2 + (50 wt% Al_2O_3–50 wt% HfO_2) mixtures heated in tungsten crucibles, black ≈ Al_2O_3, white ≈ $(U_{1-x}Hf_x)O_2$. The proeutectic UO_2 dendrites are surrounded by the eutectic phase which increases with the initial UO_2 proportion. (a) 31 wt% UO_2, (b) 40 wt% UO_2, (c) 60 wt% UO_2, (d) 70 wt% UO_2.

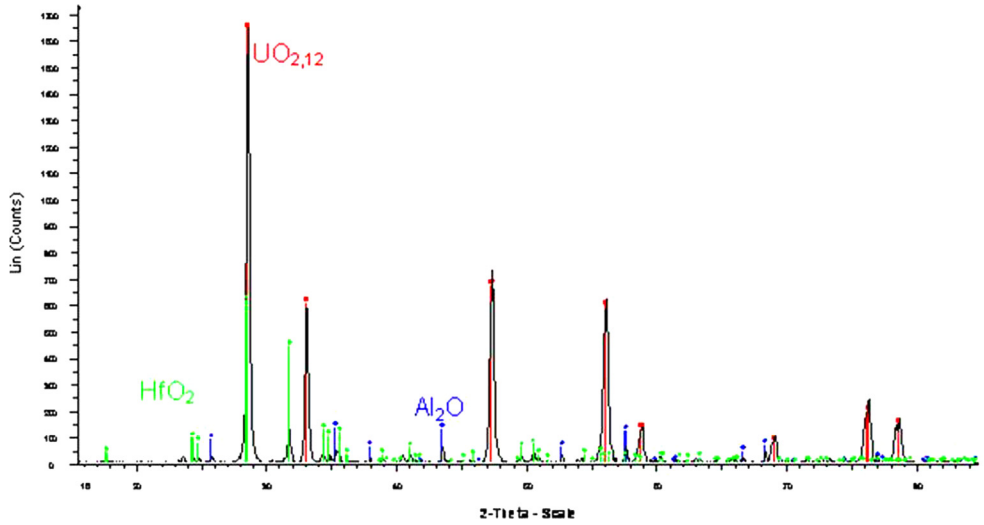

Fig. 12. X-ray diffraction of 31 wt% UO_2–34 wt% Al_2O_3–35 wt% HfO_2 sample.

Table 2
Eutectic temperatures, Liquidus temperatures and composition of the eutectic phases relative to experiments in the UO_2–(50 wt% Al_2O_3–50 wt% HfO_2) system.

Initial wt% UO_2		**31 wt%**	**40 wt%**	**60 wt%**	**70 wt%**
Liquidus temperature (°C) in the pseudo-binary UO_2–(50 wt% Al_2O_3–50 wt% HfO_2) system		1730	2093	2200	2280
Eutectic temperature (°C)		1730	1740	1755	1715
Eutectic	**UO_2**	30	35	32	
composition	**Al_2O_3**	35	36	47	/
(wt%)	**HfO_2**	35	29	21	

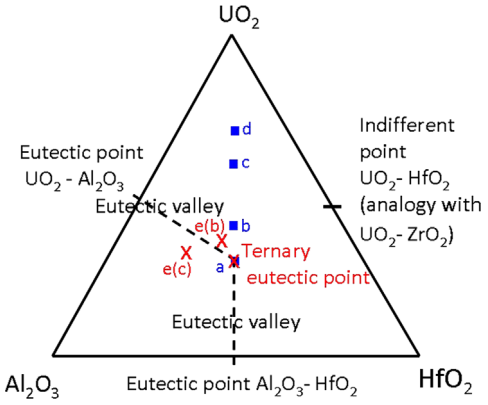

Fig. 13. Ternary UO_2–Al_2O_3–HfO_2 phase diagram (weight compositions) with the ternary eutectic point and eutectic valleys. The points determined from the experiments in the UO_2–(50 wt% Al_2O_3–50 wt% HfO_2) system were drawn on the diagram (squares = initial compositions, crosses = eutectic compositions determined by EDS.

richest sample could not be determined, being sufficiently large to be analyzed by EDS. The compositions of the eutectic zones from the samples that contained initially 40 wt% and 60 wt% UO_2 are different as the ternary eutectic composition 30 wt% UO_2–35 wt% Al_2O_3–35 wt% HfO_2. They are situated in the eutectic valley between the ternary eutectic position and the binary eutectic Al_2O_3–UO_2. A schematic ternary phase diagram with the ternary eutectic point and the eutectic valleys is drawn in Fig. 13. The binary eutectic compositions Al_2O_3–UO_2 and Al_2O_3–HfO_2 which were previously experimentally determined are positioned on this ternary phase diagram, likewise the indifferent point composition of the binary UO_2–HfO_2 system which was estimated from the UO_2–ZrO_2 system. The experimental points determined during this study are positioned on this ternary phase diagram.

A pseudo-binary phase diagram UO_2–(50 wt% Al_2O_3–50 wt % HfO_2) is proposed (Fig. 14). The four measured eutectic temperatures are extremely close (Table 2). The average eutectic temperature for the UO_2–(50 wt% Al_2O_3–50 wt% HfO_2) system is 1728 ± 22 °C. The uncertainty was calculated with Student's law, adapted to small series.

4. Conclusion

The UO_2–Al_2O_3–HfO_2 system has been investigated.

A 2030 °C melting temperature of pure alumina was measured in the VITI facility. This temperature is close to the temperature reported by the literature: 2042 °C.

Within this system, the binary eutectic positions of UO_2–Al_2O_3 and Al_2O_3–HfO_2 sub-systems were verified. They were found respectively for the following compositions (± 5 wt%) and temperatures (± 35 °C): 47 wt% UO_2 + 53 wt% Al_2O_3 and 1850 °C (2123 K) and 49 wt% HfO_2 + 51 wt% Al_2O_3 and 1800 °C (2073 K). Our measured eutectic temperatures are 65–90 °C lower than the temperatures found in the literature.

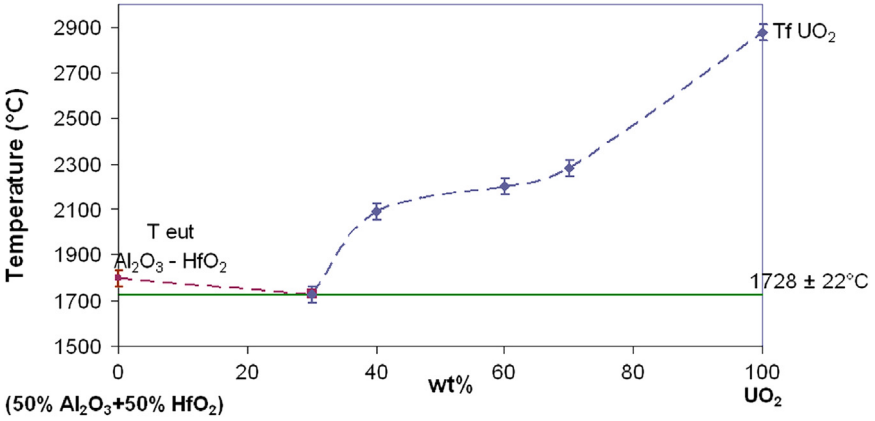

Fig. 14. Pseudo-binary UO_2–(50 wt% Al_2O_3–50 wt% HfO_2) phase diagram.

Under the experimental conditions used, under cooling or other non equilibrium effects could explain that our experimental eutectic temperatures are lower than those given in the literature.

The temperature and the composition of the ternary eutectic of the UO_2–Al_2O_3–HfO_2 system were determined: the eutectic temperature is 1728 ± 22 °C (2001 ± 22 K) and the eutectic composition (± 3 wt%) is 30 wt% UO_2–35 wt% Al_2O_3–35 wt % HfO_2. Then, a pseudo-binary UO_2–(50 wt% Al_2O_3–50 wt% HfO_2) phase diagram has been proposed.

Moreover, it is necessary to note that further investigations of this ternary system should be done to complete the study of the sacrificial material for the generation IV SFR core catcher. Knowing the UO_2–Al_2O_3–HfO_2 system it is partially possible to forecast the way the fissile part of the corium interacts with the sacrificial material. The interaction of the HfO_2–Al_2O_3 eutectic mixture with sodium shall also be studied.

Acknowledgments

This work was done within the CEA PhD grant of Kamila Plevacova, which is part of the EURATOM 7th Framework Program [FP7/2007–2011] Grant agreement no. 232658 (CP-ESFR—Collaborative Project on European Sodium Fast Reactor).

The efforts of the PLINIUS platform experimental team are gratefully acknowledged.

References

[1] S. Beils, B Carluec, N. Devictor, G.L. Fiorini, J.F. Sauvage, Safety for the future sodium cooled fast reactors, in: Proceedings of International Conference on Fast Reactors and Related Fuel Cycles FR09, Kyoto, Japan, December 7–11, 2009.

[2] K. Plevacova, Etude des matériaux sacrificiels absorbants et diluants pour le contrôle de la réactivité dans le cas d'un accident hypothétique de fusion du cœur de réacteurs de quatrième génération, Ph.D. thesis in Physics, Orleans University, France, 2010.

[3] C. Journeau, K. Plevacova, G. Rimpault, S. Poumerouly, Sacrificial materials for SFR severe accident mitigation, in: Proceedings of ICAPP'10, San Diego, CA, USA, June 13–17, 2010.

[4] S. Poumerouly, Neutronics aspects associated to the prevention and mitigation of severe accidents in sodium cooled reactor cores (Ph.D. thesis), Institut Polytechnique de Grenoble, France, 2010.

[5] S.M. Lang, F.P. Knudsen, C.L. Fillmore, R.S. Roth, High-temperature reactions of uranium dioxide with various metal oxides, National Bureau of Standards Circular (United States) 568 (1956) 1–32.

[6] L.M. Lopato, A.V. Shevchenko, G.I. Gerasimyuk, The system HfO_2–Al_2O_3, Izvestiya Akademii Nauk SSSR, Inorganic Materials 12 (9) (1976) 1331–1334.

[7] W.A. Lambertson, M.H. Mueller, Uranium oxide phase equilibrium systems: I, UO_2–Al_2O_3, Journal of the American Ceramic Society 36 (1953) 329–331.

[8] L.F. Epstein, W.H. Howland, Binary mixtures of UO_2 and other oxides, Journal of American Ceramic Society. 36 (1953) 334.

[9] P. Piluso, M. Ferrier, C. Chaput, J. Claus, J.P. Bonnet, Hafnium dioxide for porous and dense high-temperature refractories (2600 °C), Journal of European Ceramic Society. 29 (2009) 961–968.

[10] P. Piluso, J. Monerris, C. Journeau, G. Cognet, Viscosity measurements of ceramic oxides by aerodynamic levitation, International Journal of Thermophysics 23 (2002) 1229–1240.

[11] K. Plevacova, C. Journeau, P. Piluso, J. Poirier, An Experimental Study of the Effect of Boron Carbide on the SFR Corium Composition, in: Proceedings of IYNC 2010, Cape Town, South Africa, July 12–18, 2010.

[12] R. Castrejon-Garcia, J.R. Castrejon-Pita, A.A. Castrejon-Pita, Design, development, and evolution of a simple blackbody radiative source, Review of Scientific Instruments 81 (2010) 055106.

[13] K. Plevacova, C. Journeau, P. Piluso, J. Poirier, Etude du carbure de zirconium en tant que revêtement résistant au corium des réacteurs nucléaires, in: Proceedings of Matériaux 2010, Nantes, France, October 18–22, 2010.

[14] K. Plevacova, C. Journeau, P. Piluso, V. Zhdanov, V. Baklanov, J. Poirier, Zirconium carbide coating for experiments with corium related to generation II, III and IV reactors, Journal of Nuclear Materials 414 (2011) 23–31.

[15] S. Bakardjieva, M. Barrachin, S. Bechta, D. Bottomley, L. Brissoneau, B. Cheynet, E. Fischer, C. Journeau, M. Kiselova, L. Mezentseva, P. Piluso, T. Wiss, Improvement of the European thermodynamic database NUCLEA, Progress in Nuclear Energ 52 (2010) 84–96.

[16] C. Guéneau, V. Dauvois, P. Pérodeaud, C. Gonella, O. Dugne, Liquid immiscibility in a (O,U,Zr) model corium, Journal of Nuclear Materials 254 (1998) 158–174.

[17] B. Cheynet, P.Y. Chevalier, E. Fischer, Thermosuite, Calphad 26 (2002) 167–174.

[18] G. Trillon, Analyses des phases du corium par diffraction des rayons X, CEA report CEA-R-6045, 2004.